Nuclear Calibration of a Large Volume Calorimeter – 9318

S. Croft, S. Philips
Canberra Industries Inc.,
800 Research Parkway, Meriden, CT 06450, USA

E. Alvarez, K. Lambert,
Canberra UK,
B528.10 Unit 1, Harwell Campus, Didcot, OX11 0TA, UK

J. Guerault, L. Passelegue, C. Mathonat, G.Widawski
Setaram Instrumentation,
7 Rue de l'oratoire, 69300 CALUIRE, France

ABSTRACT

The non-destructive assay of canisters of Pu-contaminated wastes and residues can be rendered impractical by traditional neutron multiplicity counting techniques when the random to spontaneous fission neutron ratio is high since accidental coincidences can then swamp the correlated signal. Provided a reliable isotopic vector for the principal heat-producing radio-nuclides can be obtained, with enough Pu present and sufficient measurement time, nuclear calorimetry offers a viable alternative approach in many such cases. Given the high precision and accuracy that can be typically obtained, calorimetry has long been an important tool for nuclear material accountability. More recently the technique has also been considered for bias-defect measurements as well as application to measuring minor actinides. Indeed the need for nuclear calorimetry to serve as the gold standard in the NDA of Pu (and certain other nuclear materials) has never been greater and yet expertise and commercial availability is declining. Here, we assess the performance of a commercial off the shelf (COTS) unit to gauge the current state of the practice.

Specifically we report on the calibration of a COTS nuclear calorimeter of the twin cell design with an assay cavity of nominally 18-liter capacity. The cavity is approximately 222mm x 292mm in cross section with a height of 272mm, originally being designed to accept vitrified glass blocks, but as such has the advantage that it can accept a diverse range of item shapes and sizes. Our focus has been to establish a calibration using a Joule effect heater and to compare it with a calibration performed using certified Pu reference material. We observed a modest heater cable effect and noted an apparent container specific baseline. We examined the impact of varying the spatial heat load pattern and performed some trials with mock 3013 storage containers. The results are presented systematically and discussed in terms of measurement accuracy according to measurement scenario. We also give all numerical results for completeness.

INTRODUCTION

The thermal energy release by the radioactive decay of certain special nuclear materials can in many situations of practical importance be measured precisely and accurately against electrical or physical reference items. If the relative isotopic composition of the nuclear material is known the heat signature then can be used to quantify the amount of nuclear material present. Nuclear calorimeters have a long history and have been used for nuclear materials accountancy to good effect throughout the fuel cycle [1]. A large variety of bespoke designs have been used over the past several decades to achieve particular measurement objectives. In this work we present results obtained with a simple general purpose 'room temperature' large volume, nearly isothermal, differential calorimeter; a SETARAM Calo Series 270 [2]. The design is modular meaning that the measurement cell is readily scaleable in size [3]. The instrument used in this work had matching measurement and reference cells approximately 222mm x 292mm x 272mm (H) giving a nominal volume of about 18-liter suitable to accept a variety of container shapes and sizes. The calorimeter is maintained at a fixed temperature by water circulation in a contoured pipe and by heater

wires. The heat flow between the container wall and the external wall is used to determine the differential signal between the array of Peltier elements mounted in the symmetrical measurement and reference cells respectively.

Fig. 1. In-situ photograph of the Calo Series 270 calorimeter used.

PLUTONIUM ITEMS AND THERMAL POWER ESTIMATES

The special nuclear material used in this work was a well characterized reactor grade PuO_2 in the form of a fine powder doubly encapsulated in welded stainless steel containers. A set of ten sources were available (containing nominally 0.1, 0.5, 1, 2, 5, 7, 10, 20, 25 and 25 g of Pu respectively) and all but the lowest mass item was used in the present work. Six power levels (approximately 17 to 460 mW) with a reasonable spacing were achieved by using combinations of the nine items. For the highest power level selected six items were combined while for the other five power levels three items were used in each case so that the thermal mass remained about the same for the different combinations. The encapsulation system was the same for all of the sources and consisted of PuO_2 held firmly by a cup into the base of an inner capsule of 25mm internal diameter. The packing density of the powder is roughly $2 g.ml^{-1}$. The inner capsule was welded shut before being placed into a snuggly fitting outer capsule of 30mm outer diameter which in turn had a lid welded into place. The external length of each assembly was approximately 58mm so that a stack of three could be fitted into the calorimeter when a rod-like heat source was needed to crudely investigate spatial dependences. Otherwise the sources were measured as a cluster located close to the center of the measurement cell. To raise the sources so that the PuO_2 was roughly at the mid-plane of the cell a light-weight open-ended but inverted Al can (similar to a paint can or coffee can) was used.

In the context of this work the most important attribute of the Pu sources is their thermal output, because the heat generated within them will eventually emerge irrespective of the details of their construction. The thermal power, P, expressed in units of mW, for the six source combinations is summarized in Table I. Measurements with Pu extended over the period 5th June 2008 to 26th June 2008 and the power quoted is the average of the power calculated for these two dates. The heat output at the end date was a factor 1.000433 times greater than at the start date. It is interesting to consider the fractional contribution of the various isotopes to the power. These are approximately 0.1173, 0.2899, 0.2992, 0.0057, 0.0002 and 0.2877 in the case of $^{238\text{-}242}Pu$ and ^{241}Am respectively. Also given in Table I is the number of sources in each combination and the random uncertainty expressed as the relative standard deviation, rsd, in percent associated with weighing the mass of powder. This is based on combining in quadrature the estimated ±0.11mg (1-sigma) uncertainty in the net mass for each contributory source present in the combination. Compared to other sources of uncertainty, which will be discussed later, these are small uncertainties and so for all practical purposes do not influence the analysis and conclusions. This is fortunate in that it means we can neglect the covariance between the combinations which arises because the different combinations share sources.

Table I. Thermal power P (in units of mW) for the six Pu source combinations (A-F). Power output is the mean value of the values calculated on 5th June 2008 and 16th June 2008. Also given is the number of source capsules per combination and the random weighing uncertainty expressed as a relative standard deviation in percent.

Combination	Number of source capsules	Power, P (mW)	Random rsd (%)
A	3	17.434	0.0048
B	3	52.298	0.0016
C	3	154.34	0.00054
D	3	248.95	0.00034
E	3	348.55	0.00024
F	6	460.61	0.00026

Far more important in determining the absolute uncertainty in the power outputs are the systematic uncertainties common to all of the source combinations through the characteristics of the oxide. The uncertainty budget is given in Table II. The entries are quoted at the notional 68.26% (i.e. 1-sigma for a normal distribution) confidence level (allowing for the number of degrees of freedom where finite observations have been made).

Table II. Systematic uncertainty budget for the nuclear heat output. Contributions are quoted in relative terms at the 68.26% confidence level. The overall uncertainty listed is simply the quadrature sum of the individual relative standard deviations.

Contribution	**rsd (%)**
Specific powers	0.11
±1 day timing	0.0021
^{238}Pu half-life	0.0058
^{239}Pu half-life	0.000019
^{240}Pu half-life	0.000062
^{241}Pu half-life	0.034
^{242}Pu half-life	1.8×10^{-9}
^{241}Am half-life	0.00082
^{241}Pu β branching ratio	0.0000054
^{238}Pu abundance	0.15
^{239}Pu abundance	0.0086
^{240}Pu abundance	0.027
^{241}Pu abundance	0.027
^{242}Pu abundance	0.000047
^{241}Am abundance	0.0075
Pu/Oxide weight fraction	0.071
Balance Calibration	0.0003
Combined	**0.20**

In constructing Table II it should be noted that decay corrections for the isotopic composition since the date of the destructive analysis back in Jan 1990 have been made using half-lives and branching coefficients taken from [4]. We made one exception and that was in the choice of the ^{241}Pu half-life where we used a value of (14.33±0.03) years rather than (14.35±0.10) years based on our own review taking into account recent unpublished data. This choice reduces the uncertainty contribution from the decay correction a worthwhile amount. Specific powers for the individual isotopes were taken from ASTM C 1458-00 [5]. The individual contributions from the different nuclides to the uncertainty in the specific power of the Pu used were propagated and summed in quadrature to arrive at the single entry listed in Table II. An uncertainty of ±1 day in the time between the isotopic determinations in 1990 and the date of measurement has been included. The 0.0021% impact reflects the increasing power that comes about by the in-growth of ^{241}Am. The uncertainties in the half-life and branching ratio affect (only) the decay corrected composition and the uncertainties in the initial relative abundance impacts the mass of nuclides at the time of the

heat measurements (the specific power contribution is dealt with separately, as noted). An important contribution comes from how well the weight fraction of Pu in the oxide was determined and, as can be seen, a far less important contribution comes from the linearity of the analytical balance used to weigh the contents.

JOULE EFFECT

The thermal response of the calorimeter, $\mu V.mW^{-1}$, was also calibrated using an electrical heater made by winding a resistive wire around a metallic cylinder. The assembly is attached to a rectangular plate slightly smaller than the cross-section of the cells, and is fitted with short nylon legs. This arrangement ensures the heater is pretty much centered in the cavity. A dummy heater is placed in the reference cell although in the measurements reported here the dummy had no electrical winding and nor did it have an electrical lead passing to the outside the cell to the power connector (Fig. 2). Standard practice is to electrically calibrate without a matrix (just air) although some trials were also done with a light weight aluminum foil matrix.

The desired electrical power dissipated as heat in the Joule effect heater is set in software and measured by the system controller. The accuracy of the controller is known through factory characterization measurements against measured powers determined using an accurately calibrated and precise voltmeter and an accurately calibrated and precise ammeter. In this work we took the power reading from the controller board. Over the power range 15 to 500mW we expect this to be a fair and unbiased estimate of the true power bounded by ±0.06% based on the previous factory work (not reported here). The 1-sigma spot value is therefore likely to be less than this. Therefore, in the context of the present work the absolute uncertainty on the electrical power is superior to that which can be calculated from first principles for the Pu material by a factor of roughly four.

Fig. 2. Photograph of the Joule effect heater (left) and dummy (right) inside the calorimeter. The power cable exits through the notch.

MOCK 3013 CONTAINERS

Engineered storage containers conforming to the US DOE 3013 prescription generally consist of an inner convenience can and two welded stainless steel cans. This can-in-can-in-can approach is expected to strongly influence the heat transfer dynamics (see for example the calculations by Santi et al [6] showing, in a different setting, the impact that the packing can exert) and was something we wanted to explore directly. Since our Pu sources are already doubly encapsulated we dispensed with the convenience can and constructed a pair of mock 3013 inner and outer cans – one set for the measurement cell and one set for the reference cell. A schematic of the 3013 mock canister is given in Fig. 3 and a photograph is given in Fig. 4.

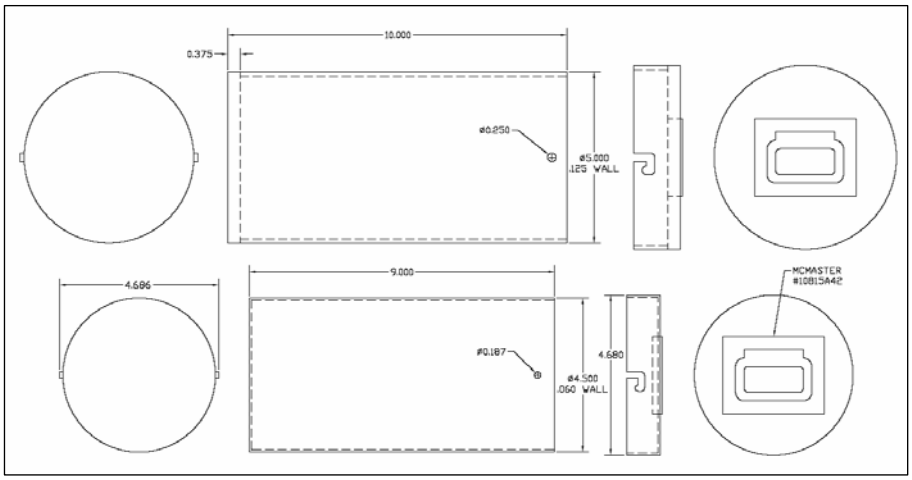

Fig. 3. Engineering sketch of the mock 3013 containers fabricated.

Fig. 4. Photograph of one of the mock 3013 containers used. The inner can is shown to the right of the un-lidded outer can.

The inner container was a cylinder 9" tall from base to open end, 4.5" OD with a wall thickness of 0.060". A cap made of the same material formed the lid. The lid had an indented spring loaded handled and attached loosely to the bottom piece by way of a pair of dog-legged slots which mated to a corresponding pair of spigots projecting from the perimeter near the rim. The outer container was of similar design but bigger. The open topped cylinder component was 10" long with a 0.375" thick base and lid. The wall thickness of the cylinder and cap was 0.125" with the OD of the bottom cylinder being 5". A similar handle and fastener were fitted.

DESCRIPTION OF EXPERIMENTS

The system was only available for a short period of time. Making productive use of the time available was therefore an important part of our activities. The delivery boxes were left in the experimental area over the weekend. They were unpacked and the system components (computer, controller, chiller, assay chamber) interconnected in a period of about 2 hours on the Monday morning. A short settling period approximately 52 hours was allowed before the first run, an overnight acquisition with the electrical heater set to the upper range of interest, was begun. We began at the upper end so that residual fluctuations would be comparatively unimportant. The upper range was set by the Pu sources available rather than by a particular application. An advantage of the differential calorimeter design is

that data collection can begin relatively quickly. The measurement series extended from June 4th 2008 until June 27th. The chronological list of the different measurements along with a brief description of each is provided in Table III in the annex. Some 35 runs were performed. Local rules meant that the Pu items could not be measured during the night or at weekends. Therefore these periods were reserved for baseline (zero power) measurements and measurements of thermal power generated by the Joule effect heater. The weekends afforded us the longest run times so that the stability of the baseline and plateaus (equilibria) at power could best be judged. Given the administrative burden of handling the Pu the daytime runs with the Pu items was typically limited to about 8 hours duration. The time to recover from the transient of opening the thermal shield to rearrange the contents of the cells and for the dynamics of the item to play out was therefore a significant part of the time available for observation. Ideally we would have liked to have carried out some runs for considerably longer (at minimum twice as long) so that equilibrium could be firmly established and subsequently monitored for long term stability. For instance we observed a tendency for the signal to overshoot very slightly (of the order of the assigned uncertainty but we nonetheless compensated for this and allowed for it in the uncertainty budget) before settling which would have a small subtle influence on results formed from a simple mathematical end point prediction algorithm working only on the rising part of the curve.

No particular care was taken to control the environmental conditions in which the calorimeter sat. The measurements were carried out in a large radiation controlled area with tall thick concrete walls but a light overhead roof with windows running around the top which allowed sunlight to stream in at dawn and strike the assay system. The area was originally designed to be used as the target area of a Van de Graaff accelerator. Industrial wall mounted heaters and coolers are installed but a large roller door to an outside compound remained in use during the measurement campaign. The temperature and humidity in the area was logged out of interest. Over a 24 h period the temperature could cycle a few ^{o}C in either direction about a nominal 21^{o}C. Throughout the period temperatures were generally in the range 19-23 ^{o}C and the relative humidity in the range 40-70%. The Pu items were stored overnight in a safe which was cooler than the experimental room. The mock 3013 containers, Joule effect heater and its dummy companion were, however, simply kept beside the calorimeter until needed. In other words, in addition to not carefully controlling the temperature of the experimental area nor did we use any form of preconditioning (preheating) of the items under study. The benefit of doing so is probably marginal, however, when one considers the time taken approaching equilibrium dominates over the initial transient phase. That said, in the interests of minimizing the disruption to the assay cells and in the hope that it may serve to shorten the transient and reduce the comparative uncertainties we did tend to follow an electrical measurement by a Pu measurement of similar power.

Both the electrical and Pu calibrations comprised 7 power values (including the zero power baseline) and followed a similar spacing so that an almost one-to-one correspondence existed. In the event of any irregularities this would have provided a diagnostic check. In the event a linear fit proved to be the most appropriate polynomial representation to both data sets. The upper power range investigated, about 450mW, was capped by the aggregate mass of Pu conveniently available. Our interest in a calorimeter of this design and size is primarily in assaying items of even higher power. Consequently we arbitrarily set a lower power cut off of about 15mW given we also wanted to include some repeat measurements as a matter of good practice and to tentatively check whether there was any dependence on the location of the heat source in the measurement cell. For this we arranged three source capsules placed one on top of the other to form what we referred to as a stack which we could place off axis.

Heat liberated within the measurement cell eventually must emerge through the faces and hence influence the embedded sensors. In this sense the signal at equilibrium is insensitive to the presence or mass of a benign matrix (i.e. one that is not undergoing a chemical or phase change for example). The rate of change of signal is matrix dependent though and in an effort to accelerate the initial transient we used Al foil, similar to baking foil in appearance, manually crumpled into low density objects roughly spherical in shape which we refer to as balls. It was hoped that the contact between the metallic balls would speed up and uniformly distribute the transport of heat from the items located in the measurement cell to the instrumented faces. The surfaces of the Al foil may be oxidized and also coated with an insulating layer of oil and so it was not obvious ahead of time that this scheme would improve matters. But because we felt it would do no harm and might reduce noise from random eddy current flow in the air (compared to having no filler) we went ahead and included Al foil in some of the runs. Within the analytical limits of these measurements we did not observe any significant difference in the quality of the assay

result with or without foil. When the Pu capsules were placed inside the double walled mock 3013 containers the heat transport is certain to be strongly determined by the coupling of the capsules to the inner container and of the inner container to the outer container. The flow of heat through the base of the containers, which are in contact with the floor of the measurement cell is likely to be an important aspect. We only performed two runs with the Pu in the 3013 cans. We used the highest power to achieve the highest signal to noise ratio above the baseline. The baseline for the 3013 canisters seemed to be measurably different than for the Joule effect heater and we therefore took disproportionately more baseline data in the case of the 3013's to make sure since we had not expected this. The evolution of the signal for the 3013's was more gradual and so a larger projection (extrapolation) was required to estimate the end point which also resulted in somewhat higher assigned uncertainties.

RESULTS

A complete summary of the numerical results may be found in the tables listed in the annex. There are five categories of results. These are: Electrical calibration with the Joule effect heaters; Pu calibration in the mid-plane performed with the various combinations of sources; the crude spatial study made with the stack of sources; the 3013 calibration; and the inverted pair measurements. The findings from each of these five studies will be discussed in subsequent sections.

An example of an electrical experiment is shown in Fig. 5. After the calorimeter is loaded there is a pronounced transient as the system responds to the severe thermal perturbation associated with having the lid opened and the measurement and reference items (which are at a different temperature than the interior) loaded. Given time the net signal will settle to a baseline value. The data acquisition is begun by the operator and is specified by setting a duration Z=(X+Y) and width Y of the electrical pulse. The software waits for a period X=(Z-Y) for the system to settle before electrical power is applied for the specified period Y. An extra period X after the electrical pulse is added automatically to allow the system to return to the baseline again. However, since we had limited time, quite often the runs were terminated early. In addition we tended to keep the settling period short so that baselines established in separate runs were averaged and recycled between analyses. In the case of electrical runs a sequence of power runs can be programmed, such as to occupy the weekend, allowing in our case two at-power pulses to be sequenced.

In the case of the Pu measurements the calorimeter was loaded and the differential signal trace logged for as long as practical. The equilibrium value was estimated including allowance for empirical projection to the end point where necessary. The base line was estimated from runs where no heat source was present. The net signal (P) is the difference, $P=(P_E-P_B)$, between the equilibrium (P_E) and baseline (P_B) values and is given in units of μV. In all cases the data are recorded in 1-second intervals which is very much shorter than the time scale of any physical transient.

Electrical Calibration

The set power was monitored by the controller and the random uncertainty was formed from the statistical scatter in the sampled data. It is much smaller than the systematic uncertainty assigned to the power setting which as already discussed was taken to have a constant fractional value independent of power setting. The uncertainty in the notional baselines corresponding to each of the runs, which were performed on different days in an area subject to normal ambient variations, is consistent with the root mean square (RMS) value of the at power uncertainty estimates. The uncertainty band assignments to the signal reflect the extrapolation uncertainty and it is not merely a model specific uncertainty (such as might be obtained based on the assumption that a single exponential profile will correctly fit the data) since a subjective contribution was also factored in.

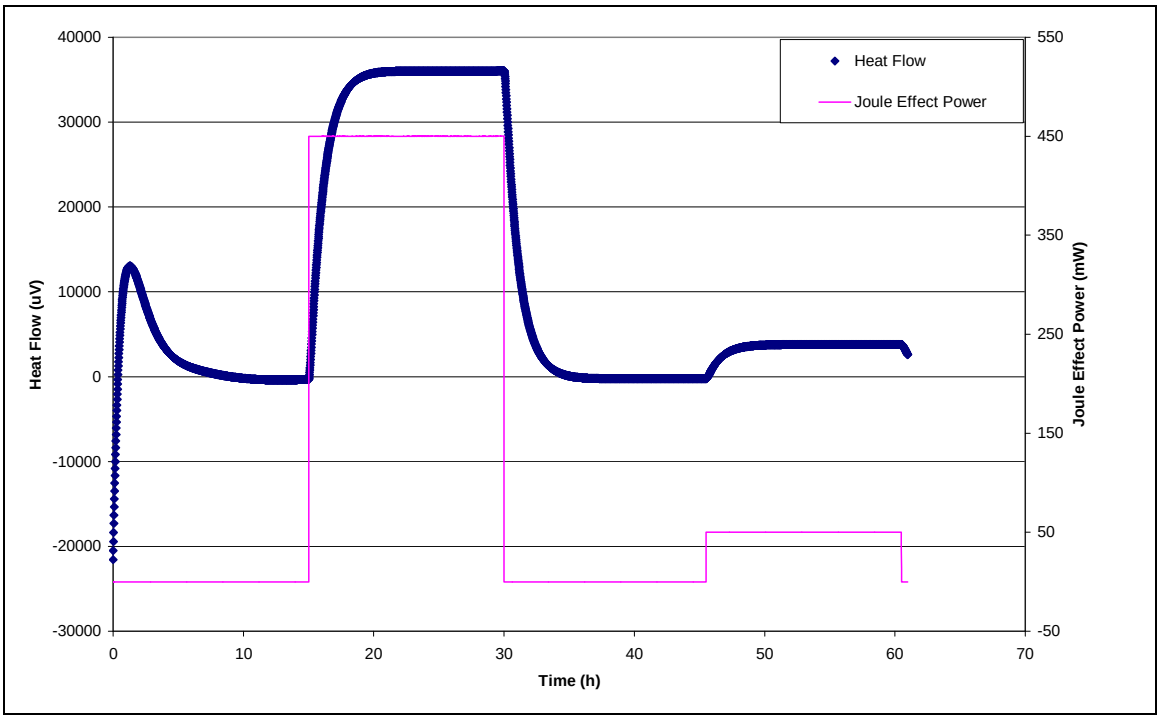

Fig. 5. Time trace of the response for a double pulse electrical calibration measurement.

A weighted linear fit to the data, gave a slope of (80.592±0.21)μV.mW^{-1} with an intercept of (-234.97±32)μV with a covariance term of -4.203. Note repeat data was appropriately averaged before fitting (so as not to wash out the aforementioned systematic uncertainties). The ratio of the Fit to the Observed signal (see Table IV) is consistent with unity within the combined uncertainty, and above a power level of about 50mW the agreement is generally within about ±0.3%. This is consistent with the fractional uncertainty of ±0.26% in the slope obtained from the fit.

Pu Calibration

The uncertainty assigned to the Pu signals observed are a little larger than for the Joule effect measurements at the same nominal power since the extrapolation to equilibrium is somewhat longer owing to the generally shorter run lengths. In the case of Pu the systematic power level is common to all points since it originates with the PuO_2 characterization. Thus, in the fitting procedure only the random (weighing) contribution is included.

A weighted linear fit to the data, gave a slope of (80.793±0.059)μV.mW^{-1} with an intercept of (19.525±5.0) μV with a covariance term of -0.1036 between them. The ratio of the Fit to the Observed signal (see Table V) is again consistent with unity within the combined uncertainties and above a power level of about 50mW the agreement is within about ±0.4%. Note repeat data was appropriately averaged before fitting.

The intercept obtained for the Pu data is significantly different to that obtained with the Joule heaters. Since the data collection was interleaved we don't think this was the result of the way the data collection was sequenced. Pending further investigation we tentatively suggest this may be a real effect associated with the fact that an electrical lead was only used to the powered heater and not to the particular dummy 'heater' used in this work thereby creating a thermal conduit between the measurement cell to the outside.

The ratio of the slope obtained from the Pu calibration to that obtained from the electrical calibration (80.793/80.592) is equal (1.0025±0.0034) where the quoted uncertainty includes the ±0.20% absolute uncertainty in the specific power level of the Pu items. This ratio is consistent with unity so that we conclude that, with the correct choice of baseline, the electrical and Pu calibrations match within the accuracy of the present experiments.

Inverted Tests

In principle we do not need to know the value of the baseline if measurements are performed in a matched pair closely spaced in time, by which we mean the item is measured twice once in the measurement cell and again in the reference cell. By reversing the roles of the two cells the signal is spread either side of the baseline so that only the spread matters and the central value become unimportant. In our case the measurements were not concurrent but we can allow for the notional baseline stability estimated from the other observations. Pu and Joule data were collected at 461 and 450mW respectively and this allows the effective calibration constant to be extracted in the vicinity of this operating point. The slope from the Joule data is (80.480±0.089) $\mu V.mW^{-1}$ and from the Pu data (80.263±0.13)$\mu V.mW^{-1}$ where the uncertainties are solely random. In forming the ratio we must also add the combined 0.21% uncertainty associated with the absolute knowledge of the electrical and Pu-thermal powers. The ratio of (0.9973±0.0029) is consistent with unity again pointing to the equivalency of the two calibrations – physical or electrical.

Stack Analysis

The purpose of the stack ('thermal rod') measurements was to investigate the dependence of the calorimeter response on the spatial distribution of heat using distributions more extreme than the difference between the Joule and Pu calibrations. Data were taken at two power levels (350mW and 154mW) each case with the sources clustered in the mid-plane and also in the form of 'thermal rods' or stacks in two different places within the measurement cell. Two locations were measured, the front right corner (FR) and the back right corner (BR). Because we have only a limited number of cases to form comparisons the statistical power of the data is admittedly weak. However, the measurement results (shown in Table VII) seem reasonably consistent against any major spatial dependence. This conclusion is also supported by the closeness of the Pu and Joule calibrations which have quite distinct heat distributions. The FR/BR ratio was found to be about (1.0056±0.0060) while the corner to center ratio was about (1.013±0.007). Although consistent with unity further investigation is warranted. In practice similarity between the items being measured would lessen any effect.

3013 Experiments

Following weighted averaging of the raw 461mW and zero power data (see Table VIII) the 3013 observations were analyzed analytically as a two point straight line fit. The slope of (81.629±0.37)$\mu V.mW^{-1}$, excluding systematic uncertainties, is a little higher than our other values but the uncertainty is also higher so consistency remains at the 2 to 3 sigma level. Given this is a single spot Pu-power determination and for the complex 3013 containers the runs are rather short in duration we consider this agreement to be fair. It is certainly encouraging that we are within 1% of the results obtained without the 3013 containment. Note the baseline for the 3013's is consistent with that observed for the other Pu experiments and again different to the Joule heater (which as noted has an electrical lead passing out of the measurement cell to a connector block).

A plot of the two 3013 runs is given in Fig. 6. The initial transients and effective start times are markedly different but the traces begin to converge as the data collection proceeds. Run 19 has about 50 minutes extra observation time over run 25 meaning that the prediction to equilibrium is marginally less.

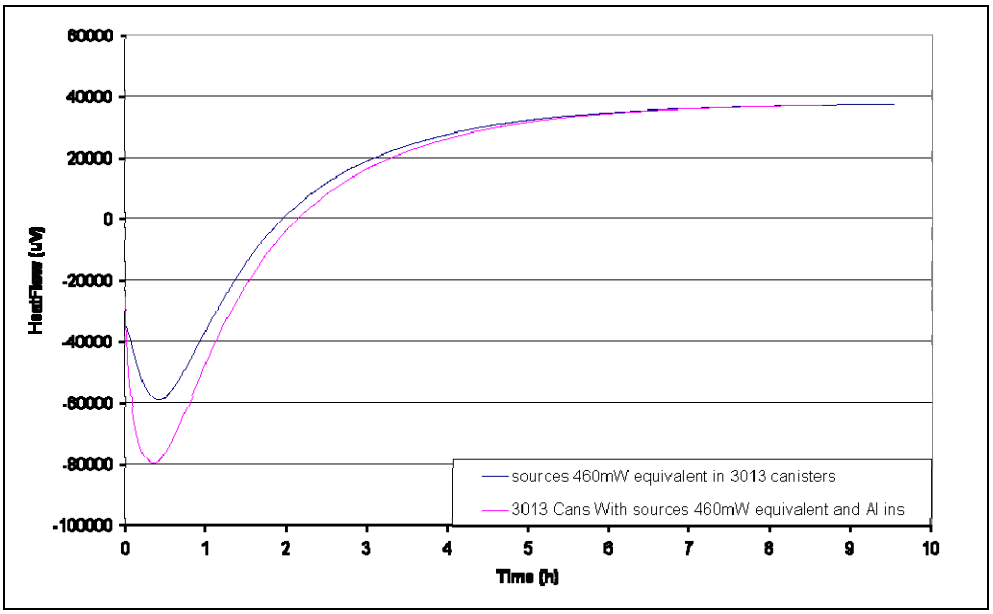

Fig. 6. Overlay of runs 19 and 25 for the 3013 container.

DISCUSION

Calorimetry can be used to measure the thermal power of nuclear items, most commonly Pu (+^{241}Am) & tritium, and in combination with knowledge of the relative isotopic composition of the contents provides a quantitative non-destructive estimate of the total Pu or tritium mass. Provided the long measurement time (compared to other non-destructive assay techniques such as quantitative gamma or combined gamma-correlated neutron) can be tolerated, calorimetry can be a relatively simple and convenient approach capable of high accuracy. The convenience and accuracy stem from the fact that for suitably designed instruments the heat measurement is essentially independent of item geometry & packaging and independent of the spatial distribution of nuclear material (heat distribution) and also self-multiplication. At equilibrium the signal is independent of the matrix material & composition provided chemical reactions such as phase changes, curing, corrosion (oxidation), rot (e.g. decomposing organic matter) and radiolysis are negligible. Furthermore electrical heat standards traceable to national standards are easy to construct and transport and may be used instead of Pu or tritium reference materials which in comparison are expensive and difficult to procure. The heat output of mixed oxide (MOX) nuclear fuel is insensitive to U and so calorimetry provides a direct assay of the Pu fraction. Baseline fluctuations depend on the environment in which the calorimeter is operated. Here differential or twin-compensation cell designs have two notable advantages - the first is the quicker settling period following set-up which come about by virtue of the signal being derived from the difference between two nominally matched cells; the second benefit is that the measurement room requires less careful control of the ambient conditions (in the present work we made no especial effort to control the temperature or humidity in the experimental hall and workaday traffic to the outside continued). It is beneficial to include a dummy in the reference cell and as we have observed the dummy heater should have an electrical lead to match the thermal connection of the actual heater in the measurement cell. As we have seen in this work with care it is possible to determine the thermal power at the 0.1% level. The accuracy of the assay may well then be limited by knowledge of the isotopic composition. For instance in the case of lean Pu residues or aged Pu the estimation of ^{241}Am content may be limiting. In the case of high burn-up Pu then the estimation of the ^{238}Pu content becomes limiting. Gold et al [7] provide a detailed account of how to evaluate uncertainties.

CONCLUSIONS

This paper summarizes a brief evaluation of a sensitive, high volume, general purpose nuclear calorimeter. We have endeavored to provide a detailed account of the experiments and furnished complete numerical results for completeness. The slope of the electrical and nuclear calibrations were compared and found to agree within experimental uncertainty which was about 0.3%. The uncertainty on the Pu heat standards was a factor of about four or so worse than for the electrical standards due to uncertainties in the nuclear data and relative isotopic

composition of the reactor grade oxide, underscoring the need for fresh and well characterized materials. A linear calibration response was observed. The impact of heat location was crudely tested by placing 'thermal rods' in the corners and comparing the results to the same sources clustered at the center of the chamber. The observations, even for these extreme configurations, were consistent at the 1 to 2 σ confidence level with no measurable effect. However, the analytical power of the data is weak and further investigation with a precision better than 0.5% is warranted. In practice, of course, using similar heat distributions to calibrate to those that are to be measured will ameliorate any residual spatial effect. The effect of a 3013 style container on thermal dynamics was studied and found to be strong but not prohibitive to making quality assays. The measurements were performed in an uncontrolled area and baseline fluctuations were observed to be important but over the power range investigated (roughly 15 to 460mW) the uncertainty introduced was tolerable. That is to say a 20 to 30μV random uncertainty in the baseline represents an uncertainty in the power of roughly 0.25mW to 0.38mW. Naturally this is more significant at the lower powers. It could probably be reduced by a factor of two quite easily, however, by controlling the ambient conditions and measuring longer (16 hours rather than 8 hours, say). For context, 15mW is the heat output from about 6g of weapons grade Pu and from about 3g of reactor grade Pu (depending on initial isotopic composition and age) The assays in the present study were limited to about 8 hours in duration because of operational constraints and longer assays are needed to reach equilibrium and establish stability directly. However, with empirical end point prediction we find that thermal results good to about ±1% were obtained for the 3013 containers at only 460mW (200g weapons grade Pu equivalent being a small amount in the context of these containers). Doubling or tripling the assay time would reduce the prediction uncertainty and sub 0.5% accuracy should be attainable even with this general purpose design. The importance of using a matched dummy in the reference cell, including electrical leads in the case of the Joule effect heater is emphasized. The electrical baseline was quite different to that observed during the Pu and 3013 containers. The difference was roughly 255μV (about 3.2mW or 1.2g of weapons grade Pu or roughly ten times the random fluctuation). It is clearly important to use the appropriate baseline if accuracy at sub percent level is to be maintained at low powers. The random baseline fluctuation of about 0.38mW represents a 1% uncertainty at a power level of 38mW which is that from about 15g of weapons grade Pu. The assay times for calorimetry proved too long to carry out meaningful replicate measurements during the present limited campaign and so this work does not have the statistical power to assess uncertainties associated with heat source distribution, item weight, heater leads, controller stability, sensitivity to the environment including vibration and electrical power, operating procedure, end-point prediction etc. Nonetheless our findings provide a good starting point for estimating the real world performance of a commercial off the shelf (COTS) system suitable for a variety of applications. Tailored designs intended for a narrower range of items types can be envisioned with improved performance in terms of precision, accuracy and instrumental response time.

ANNEX: SUMMARY OF EXPERIMENTAL RUNS AND NUMERICAL DATA

Table III. Chronological list of the measurements, by start date and time, taken in June 2008 with the Setaram Calo Series 270 large volume nuclear calorimeter.

Run	Description	Start date & time
1.	Joule heating cycle 450mW.	4th at 15:57
2.	Source combination F on top of Al can (filled with a 2m long strip of Al foil) sample cell filled with 15m of Al foil scrunched into balls. Reference cell also contains positioning can and foil. Thermal power ~461mW.	5th at 8:22
3.	Joule heating cycle 350 mW.	5th at 17:59
4.	Source combination E on top of Al can (filled with 2m long strip of foil) sample cell filled with 15m of Al foil balls. Reference cell also contains a can and foil. Thermal power ~349mW.	6th at 8:12
5.	and 6. Weekend measurement that comprises two Joule heating cycles: one at 450mW and the second one at 50mW.	6th at 16:06
6.	Continuation of 5. Note, run 5/6 also provides a baseline estimate before and a baseline after the application of electrical power. The baseline before was a little too short and needed extrapolation. The one afterwards looks quite reasonable however.	
7.	Source combination B on top of Al can (filled with 2m foil) sample cell filled with 15m Al foil balls. Reference cell also contains positioning can and foil. Thermal power ~52mW.	9th at 8:28.
8.	Joule heating cycle 150 mW.	9th at 17:52
9.	Source combination C on top of Al can (filled with 2m foil) sample cell filled with 15m Al foil balls. Reference cell also contains can and foil. Thermal power ~154mW.	10th at 8:37
10.	Joule heating cycle 50 mW.	10th at 17:22
11.	Source combination D on top of Al positioning can (filled with 2m foil) sample cell filled with 15m Al foil balls. Reference cell also contains a positioning can and foil. Thermal power ~249mW.	11th at 8:34
12.	Joule heating cycle 250 mW.	11th at 17:29
13.	Repeat measurement of case number 2. Thermal power ~461mW.	12th at 8:34
14.	Joule heating cycle 15 mW.	12th at 8:15
15.	Sources combination A on top of Al can (filled with 2m foil) sample cell filled with 15m Al foil balls. The reference cell also contains a support can and foil. Thermal power ~17.4mW.	13th at 8:39
16.	Weekend measurement with Al cans and foil but no sources. Thermal power is zero. This run is a good baseline for the Pu calibration.	13th at 17:14
17.	Stack with source combination E surrounded in 4m of foil place on right front corner of the sample cell, cell filled with 15m foil. Similar setup in reference cell. Thermal power ~349mW.	16th at 8:50
18.	3013 Canisters with 5 Al cans inside. Cells filled with foil. No sources. Thermal power is zero. One of several 3013 baseline runs.	16th at 17:58
19.	3013 Canisters with 5 Al cans inside and source combination F on top of them. Cells filled with foil. Thermal power ~461mW.	17th at 8:46
20.	Joule heating elements inside the measurement cells. No power was applied although it was supposed to come up to 450mW. The Reference and Sample cells had been switched around (as an inversion experiment) but inadvertently the electrically connections had not been flipped so that no thermal power was actually applied. This run should in principle serve as an additional baseline measurement but equilibrium was never achieved and so it was not used in the	17th at 18:34

	analysis.	
21.	Source combination F on top of Al can (filled with 2m foil) sample cell filled with 15m Al foil balls. Reference cell also contains a positioning can and foil. The Reference and Sample cells were inverted as a check on symmetry of the differential system and so that we may use paired measurements to extract the power. Thermal power ~461mW.	18th at 8:54
22.	Joule heating cycle 450mW. Reference and sample cells inverted to provide an electrical analog to match run number 21.	18th at 17:53
23.	Stack with source combination E surrounded in 4m of foil place on right back corner of the sample cell, measurement cell was filled with 15m of Al foil. Similar setup in reference cell. Thermal power ~349mW.	19th at 8:44
24.	3013 Canisters with 5 small Al-cans inside. Cells filled with foil. No sources. Zero thermal power.	19th at 17:41
25.	3013 Canisters with 5 small Al-cans inside and source combination F on top of them. Cells filled with foil. Thermal power ~461mW. This is essentially a repeat of run 19 but the thermal perturbation of loading the items and the duration are of course different. The signal converges with that of run 19 rather nicely towards the end of the run but run 19 extends for about 50 minute longer somewhat easing the projection to equilibrium.	20th at 8:49
26.	3013 Canisters with 5 small Al-cans inside. Cells contain no foil. No Pu sources. Zero power baseline run.	20th at 17:42
27.	Stack with source combination C surrounded in 4m of foil place on right front corner of the sample cell, cell filled with 15m foil. Similar setup in reference cell. Thermal power ~154mW.	23rd at 8:59
28.	Joule heating cycle 450mW, with foil filling the cells.	23rd at 17:50
29.	Stack with source combination C surrounded in 4m of foil place on right back corner of the sample cell as viewed from the open lid, cell filled with 15m foil. Similar setup in reference cell. Thermal power ~154mW.	24th at 8:56
30.	Baseline measurement, zero thermal power, with Al positioning cans and Al foil but no Pu sources.	24th at 8:56.
31.	Source combination B on top of Al can (filled with 2m foil) sample cell filled with 15m Al foil balls. Reference cell contains can and foil as well. This is a repeat measurement to case number 7. Thermal power ~52mW.	25th at 8:58.
32.	Baseline, zero power, with Joule heaters in place, no Al foil.	25th at 17:36.
33.	As per case number 11. Thermal power ~249mW.	26th at 8:56.
34.	3013 Canisters with 5 small Al-cans inside. Cells filled with Al foil. No sources. Thermal power is zero so this is another 3013 baseline measurement.	26th at 17:24.
35.	Baseline, thermal power of zero, with Joule heaters in place and electrical cable connected, no Al foil. Reference and sample cells inverted (i.e. the heater is in the reference cell and the dummy is in the sample measurement cell) as a baseline check in the symmetrical arrangement corresponding to run 22. Equilibrium was not established and so this run was not used in subsequent analysis of the data.	27th at 15:11.

Table IV. Electrical Calibration data.

Run #	Power (mW)	Overall Unc.[a] (%)	Overall Unc. (mW)	Signal (□V)	Band (□V)	Base Line (□V)	Total (□V)	Fit (□V)	Unc. (□V)	Fit/Obs. (Ratio)	Unc. in Ratio
1	450.13	0.08	0.36010	35930	24	24	33.9	36041.9	82.6	1.003115	0.002485
5	450.05	0.07	0.31504	36010	30	24	38.4	36035.5	81.3	1.000707	0.002498
28	449.86	0.08	0.35989	36175	30	24	38.4	36020.1	82.5	0.995719	0.002514
3	350.03	0.08	0.28002	27890	22	24	32.6	27974.6	62.3	1.003035	0.002521
12	249.88	0.08	0.19990	19940	28	24	36.9	19903.4	43.4	0.998162	0.002854
8	149.87	0.09	0.13488	11980	30	24	38.4	11843.4	29.4	0.988594	0.004007
6	49.99	0.08	0.03999	3796	10	24	26.0	3793.8	27.1	0.999427	0.009890
10	49.99	0.08	0.03999	3818	16	24	28.8	3793.8	27.1	0.993668	0.010331
14	14.98	0.07	0.01049	905	20	24	31.2	972.3	30.3	1.074363	0.049999
5	0	0	0	-237	12	0	12.0	-235.0	32.2	0.991435	0.144818
5	0	0	0	-290	80	0	80.0	-235.0	32.2	0.810241	0.249566
20	0							Not used			

[a] The 'overall uncertainty' (Unc.) is formed from the direct sum of the relative standard deviation (in %) and the bias (0.06% taken to be the same value for all power measurements). Baseline experiments naturally do not have additional baseline uncertainty allowances.

Table V. Pu Calibration data.

Run #	Power (mW)	Overall Unc.[a] (%)	Overall Unc. (mW)	Signal (□V)	Band (□V)	Base Line (□V)	Total (□V)	Fit (□V)	Unc. (□V)	Fit/Obs.	Unc.
2	460.61	0.00026	0.00119759	37335	50	30	58.3	37233.6	25.8	0.997284	0.001704
13	460.61	0.00026	0.00119759	37105	33	30	44.6	37233.6	25.8	1.003466	0.001393
4	348.55	0.00024	0.00083652	28190	35	30	46.1	28179.9	19.4	0.999643	0.001773
11	248.95	0.00034	0.00084643	20165	35	30	46.1	20132.9	13.8	0.998410	0.002382
33	248.95	0.00034	0.00084643	20045	40	30	50.0	20132.9	13.8	1.004387	0.002598
9	154.34	0.00054	0.00083344	12489	16	30	34.0	12489.1	8.7	1.000009	0.002810
7	52.298	0.0016	0.00083677	4292	30	30	42.4	4244.8	4.9	0.989011	0.009842
31	52.298	0.0016	0.00083677	4235	30	30	42.4	4244.8	4.9	1.002323	0.010107
15	17.434	0.0048	0.00083683	1459	15	30	33.5	1428.1	4.7	0.978801	0.022735
16	0	0	0	13	12	0	12.0	19.5	5.0	1.501923	1.438859
30	0	0	0	19	12	0	12.0	19.5	5.0	1.027632	0.700455

[a] The 'overall uncertainty' is the relative standard deviation (expressed in %) with no bias added.

Table VI. Inverted Tests data.

Run #	Power (mW)	Overall Unc.[a] (%)	Overall Unc. (mW)	Signal (□V)	Band (□V)	Base Line (□V)	Total (□V)
Pu:							
2, 13	460.61	0.00026	0.00119759	37190			111.0
21	460.61	0.00026	0.00119759	-36750	40	30	50.0
35	0	0	0	200	100	30	104.4
Joule:							
1, 5, 28	450.01	0.07	0.315007	36028			72.0
22	450	0.08	0.36	-36405	25	24	34.7

[a] The 'overall uncertainty' is formed from the direct sum of the relative standard deviation (in %) and the bias (0.06% for all electric calibration measurements and 0% for the Pu measurements). A baseline is not needed to analyze the Inverted Test data because the signal is split approximately symmetrically about the baseline such that only the spread matters.

Table VII. Stack Analysis with Pu at both 349mW and 154mW.

Run #	Power (mW)	Overall Unc.[a] (%)	Overall Unc. (mW)	Signal (□V)	Band (□V)	Base Line (□V)	Total (□V)
4	348.55			28190	35	24	42.4
17				28625	50	24	55.5
23				28568	30	24	38.4
Weighted by Total Uncertainty Mean:				28445			25.0[b]
							191.0[c]
							135.0[d]
9	154.34			12489	16	24	28.8
27				12725	25	24	34.7
29				12530	25	24	34.7
Weighted by Total Uncertainty Mean:				12569			19 [b]
							191 [c]
							135 [d]

[a] The 'overall uncertainty' is the relative standard deviation (expressed in %) with no common bias added.
[b] Internal Standard Error.
[c] External Standard Deviation.
[d] External Standard Error.

Table VIII. 3013 experiments with Pu at a power level of 461mW.

Run #	Power	Overall Unc.[a]	Overall Unc.	Signal	Band	Base Line	Total
	(mW)	(rsd%)	(mW)	(□V)	(□V)	(□V)	(□V)
19	460.61	0.00026	0.00119759	37582	210	20	211.0
25	460.61	0.00026	0.00119759	37673	280	20	280.7
18	0			-52	60		
24	0			12	12		
26	0			20	10		
34	0			16	6		

[a] The 'overall uncertainty'(Unc) is the relative standard deviation (rsd) (expressed in %) with no bias added. Baseline determinations do not have additional baseline uncertainties whereas assay experiments do because they are taken on different days.

REFERENCES

1. ANSI N15.22-1987, "American National Standard for nuclear materials – Plutonium-bearing solids calibration techniques for calorimetric assay", Publ. by ANSI, Inc., 1430 Broadway, New York, NY 10018.
2. J. GUERAULT, C. MATHONAT, G. ETHERINGTON, and S. CROFT, "Factory assessment of large volume nuclear calorimeters", Proc. 49th Annual meeting of the INMM (Institute of Nuclear Materials Management), July 13-17 2008, Nashville, Tennessee, USA. CD-ROM produced by Omnipress (2008).
3. C. MATHONAT and J-F. MAUGER, "Large volume and high sensitivity calorimetry for nuclear materials investigations", Proceeding ESARDA (2007).
4. R.B. FIRESTONE, "Table of Isotopes Eighth Edition", Volume II, John Wiley and Sons, Inc. (1996). ISBN 0-471-14917-9.
5. ASTM C 1458-00, "Standard test method for nondestructive assay of plutonium, tritium and ^{241}Am by calorimetric assay", ASTM Book of ASTM Standards 2004, Section 12, Volume 12.01 Nuclear Energy (I) (2004)911-925, ISBN 0-8031-3756-7.
6. P.A. SANTI, D.S. BRACKEN, D.A. MACARTHUR and M.K. SMITH, "Use of fast calorimetry to perform mass attribute measurements", Los Alamos National Laboratory Report LA-UR-07-3752 (2007), Presented at 48th Annual Meeting of the INMM, Tucson, AZ, USA, July 8-12, 2007.
7. A.S. GOLD, P. DE RIDDER and G. LASZLO, "Comparison between calorimeter and HLNCC errors", 32nd Annual Meeting Proceedings, New Orleans, LA, USA July 28-31, 1991, Nuclear Materials Management XX(1991)767-770.